Eur. Phys. J. D **43**, 113–116 (2007)
DOI: 10.1140/epjd/e2007-00079-7

THE EUROPEAN PHYSICAL JOURNAL D

Dynamics of atom scattering from ^{4}He nanoclusters

E. Krotscheck[1,a] and R.E. Zillich[1,2]

[1] Johannes Kepler Universität, Linz 4040, Austria
[2] Fraunhofer ITWM, Fraunhoferplatz 1, 67663 Kaiserlautern, Germany

Received 23 July 2006 / Received in final form 22 September 2006
Published online 24 May 2007 –

Abstract. We present a microscopic theory and results of atom scattering calculations to determine the dispersion of surface modes (ripplons) of superfluid helium-4 nanodroplets, expanding previous work [J. Chem. Phys. **115**, 10161 (2001)]. A quantum transport formalism is adapted to the many-body scattering problem, yielding both elastic and inelastic fluxes. We demonstrate that, in analogy to the dynamic structure function $S(k,\omega)$ obtained from neutron scattering, a dynamic structure function $\sigma(k,\omega)$ can be obtained from ^{3}He scattering. The ^{3}He dynamic structure function $\sigma(k,\omega)$ is sensitive to surface dynamics, whereas the neutron dynamic structure function $S(k,\omega)$ is dominated by bulk-like excitations, in particular by rotons. Unlike for neutron-scattering, the total inelastic cross section for atom-scattering on ^{4}He nanodroplets is large which we believe makes experimental detection feasible. We also show that scattering *identical* particles, i.e. ^{4}He atoms, does not provide information about the dispersion of surface modes. Instead, inelastically scattered ^{4}He atoms preferably lose roughly half their energy.

PACS. 36.40.-c Atomic and molecular clusters – 67. Quantum fluids and solids; liquid and solid helium

1 Introduction

Superfluid ^{4}He nanodroplets have found use for spectroscopy of molecules and complexes which are cooled to 0.3–0.4 K by the ^{4}He environment while the main spectral features are not altered. The solvation structure and the dynamics of dopants in ^{4}He have been investigated experimentally and theoretically [2,3], they are overall well understood. The process of capturing an atom or a molecule in ^{4}He droplets, i.e. inelastic scattering/absorption off/by ^{4}He droplets is less well understood. We present correlated basis function (CBF) calculations of the scattering cross section of ^{3}He atoms and compare to ^{4}He scattering cross sections. In the present work, which complements a previous study on this topic [1], we focus on the possibility to use atom-droplet scattering to probe excitations in the droplets. The methods presented below are immediately applicable to ultra-cold atomic gases in the regime of Feshbach-resonance enhanced interactions. Advances of experimental techniques should make such scattering experiments feasible.

2 Theory

We give a brief overview of the calculation of excited states of a non-uniform many-boson system (pure and with impurities) using CBF theory. A full description can be found in references [1,4]. Let Ψ_0 be the N-body ground state of the microscopic Hamiltonian $H = T + V$, where V is the 2-body interaction operator. The wave function of the perturbed system is written as

$$\Psi(t) = \frac{e^{\delta U(t)/2}\Psi_0}{\langle\Psi_0|e^{\Re e\, U(t)}|\Psi_0\rangle}$$

$$\delta U(t) = \sum_{i=1}^{N} \delta u_2(\mathbf{r}_i;t) + \sum_{i<j} \delta u_2(\mathbf{r}_i,\mathbf{r}_j;t) + \ldots$$

We determine the fluctuations by an action principle: we define an action integral with respect to $\Psi(t)$ as

$$\mathcal{S} = \int_{t_1}^{t_2} dt\ \langle\Psi(t)|H + U^{(\mathrm{ext})}(t) - i\hbar\frac{\partial}{\partial t}|\Psi(t)\rangle = 0. \quad (1)$$

Demanding stationarity of $\mathcal{S}$ with respect to all components of the excitation operator $\delta U(t)$,

$$\frac{\delta\mathcal{S}}{\delta u_1^*(\mathbf{r}_0;t)} = 0, \quad \frac{\delta\mathcal{S}}{\delta u_2^*(\mathbf{r}_0,\mathbf{r}_1;t)} = 0, \quad \ldots \quad (2)$$

is equivalent to the time-dependent Schrödinger equation. Fluctuations that involve simultaneously n particles decrease in importance with increasing n, therefore triplet correlations δu_3 and higher correlations are neglected. The resulting time-dependent coupled equations for δu_1 and δu_2 can be linearized in the limit of weak external potential $U^{(\mathrm{ext})}(t)$. These coupled linear equations of motion are then solved approximately [1].

[a] e-mail: eckhard.krotscheck@jku.at

Specifically for a scattering situation, the equations of motion can be written as a single-particle wave equation with a non-local, non-Hermitian, energy-dependent self energy Σ (expressed in terms of ground state quantities, see Ref. [1])

$$-\frac{\hbar^2}{2m_X}\frac{1}{\sqrt{\rho_1^X(\mathbf{r})}}\nabla\rho_1^X(\mathbf{r})\nabla\frac{1}{\sqrt{\rho_1^X(\mathbf{r})}}\,\varphi_\omega(\mathbf{r}) + \int d^3r'\,\Sigma(\mathbf{r},\mathbf{r}';\omega)\varphi_\omega(\mathbf{r}') = \hbar\omega\int d^3r'\,S(\mathbf{r},\mathbf{r}')\varphi_\omega(\mathbf{r}'), \tag{3}$$

where X stands for either ^{4}He or ^{3}He, $\rho_1^X(\mathbf{r}) = \rho_1^X(r)$ is the respective ground state probability density, $S(\mathbf{r},\mathbf{r}')$ is the static structure function in the ^{4}He case and $\delta(\mathbf{r}-\mathbf{r}')$ in the ^{3}He case, and $\varphi_\omega(\mathbf{r})$ is the *elastic* channel wave function for an incident particle of energy $E = \hbar\omega + \mu_X$, where μ_X is the chemical potential of species X. Asymptotically, $\varphi_\omega(\mathbf{r})$ has the usual scattering form

$$\varphi_\omega(\mathbf{r}) \to e^{i\mathbf{kr}} + f(\theta)e^{ikr}/r. \tag{4}$$

From $\varphi_\omega(\mathbf{r})$ we can calculate elastic cross sections $\sigma_{\rm el}$ and total inelastic cross sections $\sigma_{\rm inel}$ (i.e. what is missing from the elastic channel). For more information about the dynamics of inelastic processes we need to calculate transport currents, as outlined in the following section.

3 Quantum transport

For the calculation of inelastic transport currents, we have to expand the expectation value of the current operator $\hat{\mathbf{j}}^I(\mathbf{r}_0)$ to *second* order in the correlations $\delta U(t)$, since in first order, it carries no net particle flux

$$\mathbf{j}^{(2)}(\mathbf{r}_0) = \frac{1}{4}\frac{\langle\Psi^I_{N+1}|\,\delta U^*\,\hat{\mathbf{j}}^I(\mathbf{r}_0)\,\delta U\,|\Psi^I_{N+1}\rangle}{\langle\Psi^I_{N+1}\mid\Psi^I_{N+1}\rangle} \tag{5}$$

$$= \mathbf{j}^{(2)}_{\rm el}(\mathbf{r}_0;t) + \mathbf{j}^{(2)}_{\rm inel}(\mathbf{r}_0;t). \tag{6}$$

Analysis of the asymptotic behavior of inelastic currents $\mathbf{j}^{(2)}_{\rm inel}$ allows the calculation of inelastic *scattering* $\sigma_{\rm insc}$ and *adsorption* $\sigma_{\rm ad}$ cross sections, and also differential cross sections, such as the angular dependence of inelastically scattered particles, $d\sigma_{\rm insc}/d\Omega$, their energy distribution, $d\sigma_{\rm insc}/dE_{\rm out}$, etc. Of particular interest are cross sections which probe the ^{4}He droplet properties, such as the probability $\sigma(k_t, E_t)$ for a particle (incident energy $E_{\rm in}$, momentum $\mathbf{k}_{\rm in}$) to transfer energy E_t and momentum k_t

$$E_t = E_{\rm in} - E_{\rm out}\,, \qquad k_t \;=\; |\mathbf{k}_{\rm in} - \mathbf{k}_{\rm out}|$$

to the ^{4}He droplet. $\sigma(k_t, E_t)$ is the atom scattering analog to the dynamic structure function $S(k,\omega)$ which is measured by neutron scattering. Details on how to explicitly calculate asymptotic currents from the definition (5) can be found in reference [1].

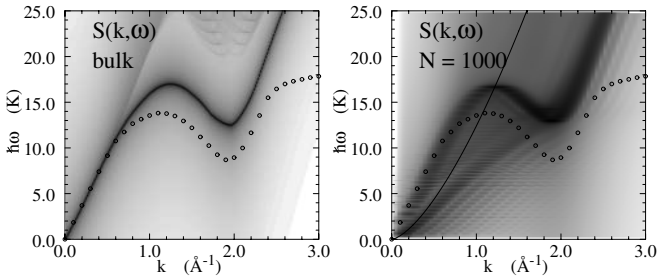

Fig. 1. Calculated dynamic structure function $S(k,\omega)$ of bulk ^{4}He (left) and of a droplet ^{4}He$_{1000}$ (right), on a log-scale. The circles represent the experimental phonon-roton spectrum in bulk ^{4}He. The line in the right panel is the ripplon dispersion of a free helium surface $\omega^2(k) = \sigma k^3/m_4\rho_\infty$, where σ is the surface energy and ρ_∞ the equilibrium density.

4 Results

We have calculated elastic and inelastic cross sections of ^{4}He and ^{3}He scattering off ^{4}He nanodroplets up to sizes of $N = 1000$. Results for total (i.e. non-differential) cross sections have been published in reference [1]. We focus here instead on differential cross sections, with emphasis on the determination of dynamic properties (dispersion relations) of the ^{4}He droplet by atom scattering. For bulk ^{4}He as well as for ^{4}He films, these properties, manifested in the dynamic structure function $S(k,\omega)$, have been measured by neutron scattering [5,6]; the same type of experiments for ^{4}He nanodroplets is experimentally very difficult. Nonetheless, $S(k,\omega)$ was calculated for droplets with CBF theory [7]. In Figure 1 we compare $S(k,\omega)$ for bulk ^{4}He and for a droplet ^{4}He$_{1000}$. Comparison with $S(k,\omega)$ measured in bulk (in Fig. 1, the experimental bulk dispersion is shown [5]) indicates that CBF theory overestimates the energies but is a significant improvement to the Bjil-Feynman spectrum [8]. $S(k,\omega)$ of a ^{4}He$_{1000}$ droplet is shown in the right panel of Figure 1. The phonon-roton branch of the droplets can be clearly seen (broadened by confinement) as well as the lower-lying surface wave (ripplon) excitations. For both bulk ^{4}He and droplets, $S(k,\omega)$ is found to be dominated by rotons.

The neutron scattering cross section $S(k,\omega)$ has to be compared to the cross section $\sigma(k_t, E_t)$. $\sigma(k_t, E_t)$ for ^{3}He is shown in Figure 2 for four droplet sizes $N = 112; 400; 700; 1000$. Firstly, we observe that, after appropriate scaling by the respective total cross section proportional to the cross sectional area, the N-dependence is weak apart from the lowest energy features, which are caused by the excitation of ripplons. The energy and momentum dependence of $\sigma(k_t, E_t)$ is evidently different from $S(k,\omega)$, for which ripplon, phonon, and roton excitations could be readily identified (right panel of Fig. 1). Unlike for $S(k,\omega)$, there is no particularly strong signal in $\sigma(k_t, E_t)$ which we can identify with the roton excitation (which from $S(k,\omega)$ we know to be present in ^{4}He droplets down to small sizes [7]). However, we will show further below that there is a small increase in $\sigma(k_t, E_t)$ at the roton energy.

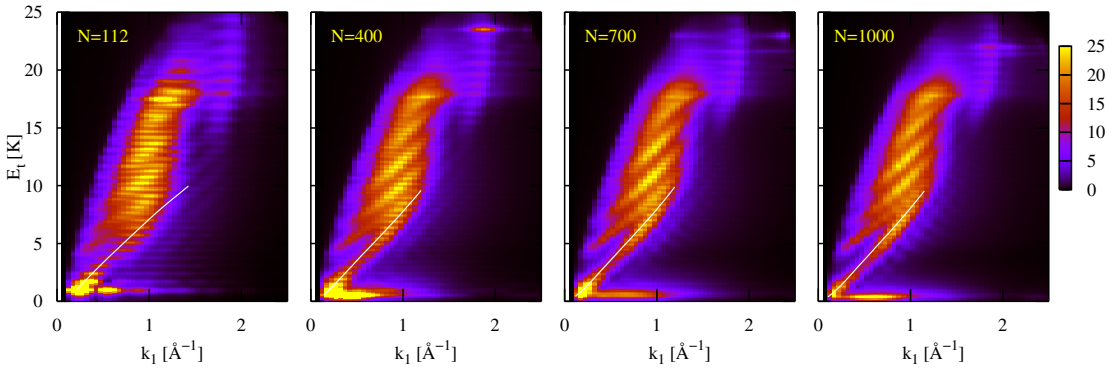

Fig. 2. (Color online) $\sigma(k_t, E_t)$ of ^{3}He scattering at ^{4}He$_N$ (incident energy $E = 26$ K), for $N = 112; 400; 700; 1000$. For comparison, the respective ripplon dispersion is shown with a line. $\sigma(k_t, E_t)$ has been broadened by $\Delta E_t = 0.2$ K, and scaled by the cross section ratio $(N_{\rm ref}/N)^{2/3}$ relative to the largest droplet, $N_{\rm ref} = 1000$.

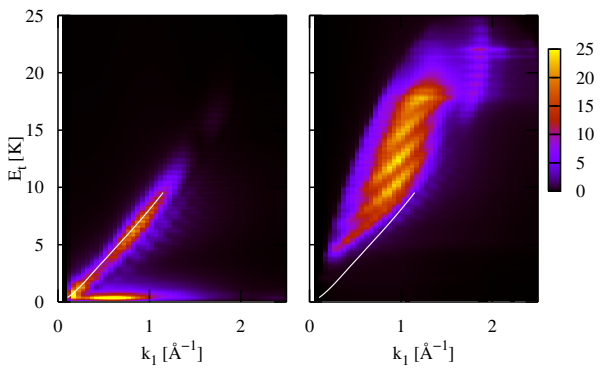

Fig. 3. (Color online) $\sigma(k_t, E_t)$ of ^{3}He scattering at ^{4}He$_{1000}$, separated into ripplon (left) and the other contributions (right).

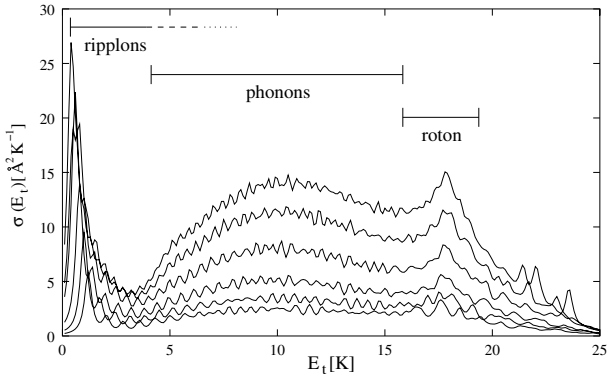

Fig. 4. The cross section for energy transfer $\sigma(E_t)$ for ^{3}He scattering at ^{4}He$_N$, is shown for incident energy $E = 26$ K, $N = 70; 112; 200; 400; 700; 1000$, where the higher curves correspond to larger N.

To relate the low-lying excitation in Figure 2 to the ripplons, we first have to express droplet excitations, which are quantized by the angular momentum ℓ, in terms of the linear momentum quantum number k. This is achieved through $k^2 = 3\ell(\ell+1)/(5r_{\rm rms}^2)$, where $r_{\rm rms}$ is the *rms* radius of the droplet. The ripplon dispersion thus obtained is show as a line for each size N in Figure 2. This comparison shows that with increasing N, $\sigma(k_t, E_t)$ becomes sensitive to ripplons, and reproduces correctly the ripplon dispersion relation. To demonstrate this we have separated the contributions to $\sigma(k_t, E_t)$ coming from exciting ripplons and from higher excitations in Figure 3 — something which is easy in an analytic theory like the CBF theory, but would not be possible in an experiment where only the complete cross sections of Figure 2 would be measured.

Finally, we note that the phonon dispersion cannot be determined from $\sigma(k_t, E_t)$. Instead we observe an interference pattern independent of N that needs further analysis for a full understanding.

The cross section $\sigma(E_t)$, i.e. the probability that the impinging atom scatters inelastically and transfers energy E_t to the ^{4}He droplet, is obtained by integrating $\sigma(k_t, E_t)$ over k_t. In Figure 4 we show $\sigma(E_t)$ for ^{3}He (incident energy 26 K) scattered at ^{4}He droplets between sizes $N = 70$ and $N = 1000$. At low transfer energies, we see the signature of the large cross section for ^{3}He-ripplon scattering; the information about the ripplon dispersion is of course lost after integrating over the momentum. For intermediate transfer energies we see a broad band of phonon scattering events. Then, around 17–18 K, there is a small peak for all but the smallest sizes. This is the energy of the roton, which is higher than the true roton energy due to approximations employed in our implementation of the CBF method. Hence, despite some lack of quantitative agreement, $\sigma(E_t)$ shows that ^{3}He also couples to the roton, albeit with smaller probability than to the ripplon.

Up to now, we have only considered impurity (^{3}He) scattering, motivated by its analogy to neutron scattering cross sections. What about ^{4}He scattering? The interaction between ^{3}He and ^{4}He is the same as among ^{4}He atoms, and the mass difference is only 25%. We expect qualitative differences between ^{3}He and ^{4}He cross sections of ^{4}He droplets because of Bose symmetry, see also the equation for the elastic channel wave function (3). Indeed, the energy-momentum transfer probability $\sigma(k_t, E_t)$ turns out to be less structured, and is not shown here. In particular, $\sigma(k_t, E_t)$ shows basically no k_t dependence, thus ruling out the possibility to obtain dispersion information from $\sigma(k_t, E_t)$ for ^{4}He scattering. In order to obtain

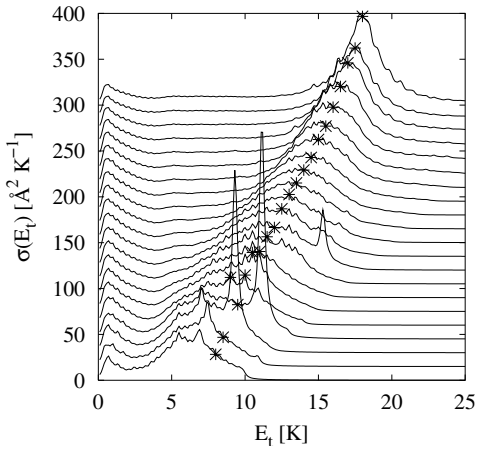

Fig. 5. The cross section for energy transfer $\sigma(E_t)$ for ^{4}He scattering at $^4\mathrm{He}_{1000}$, for incident energies $E = \hbar\omega + \mu_X$, $\hbar\omega = 16; 17; 18; \ldots; 36$ K. $\sigma(E_t)$ is offset for growing energy for better visibility. The star indicates $\sigma(E_t)$ at half the incident energy, $E_t = \hbar\omega/2$.

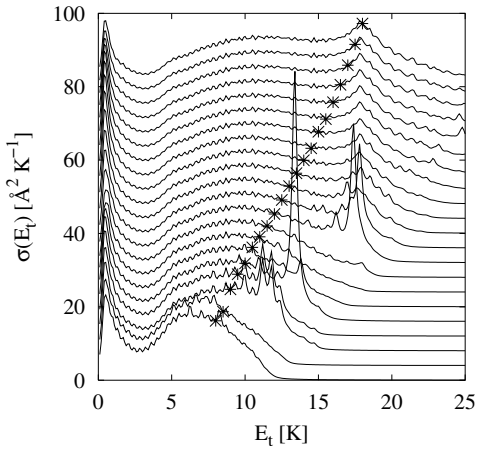

Fig. 6. Same as Figure 5 for ^{3}He scattering.

energy-related features, we have calculated $\sigma(E_t)$. In Figure 5, we show $\sigma(E_t)$ for ^{4}He scattering at a large droplet, $^4\mathrm{He}_{1000}$, for incident energies between 16 K and 36 K. Figure 6 shows the corresponding result for ^{3}He scattering for comparison. As for ^{3}He scattering, a high cross section for ripplon scattering can be observed for ^{4}He scattering which saturates with increasing incident energy. Interestingly, for ^{4}He scattering $\sigma(E_t)$ lacks features related to roton coupling, although we point out that the roton can be detected in the elastic cross section σ_{el} (see Ref. [1]). Instead, with increasing energy, $\sigma(E_t)$ becomes peaked at *half* the full incident energy (i.e. including the chemical potential, $\hbar\omega = E - \mu_4$) of the ^{4}He atom, at $E_t = \hbar\omega/2$ (indicated by a star in Fig. 5). That means the incident energy is preferably split in half, shared by two out-going ^{4}He atoms. It will be interesting to investigate the angular dependence of $\sigma(E_t)$, $d\sigma(E_t)/d\Omega$, in search for interference effect due to Bose symmetry and for an explanation of the peak at $E_t = \hbar\omega/2$. This result for ^{4}He scattering is in contrast to the result for ^{3}He scattering discussed above and shown in Figure 6 for $N = 1000$, where $\sigma(E_t)$ is distributed widely and no peak is found at $E_t = \hbar\omega/2$. Instead, a small peak at the energy of the roton develops and saturates with increasing incident energy. We finally note that for certain incident energies, $\sigma(E_t)$ can exhibit resonances, as evidenced by sharp peaks. Discussion of these details of $\sigma(E_t)$ is beyond the scope of the present paper.

For scattering experiments with ^{4}He droplets, the size distribution [9] of droplets generated by expansion from a nozzle has to be taken into account. As evident from Figure 2, the N-dependence of $\sigma(k_t, E_t)$ is essentially just a proportionality to the cross sectional area, therefore the size distribution is no impediment to measuring $\sigma(k_t, E_t)$. The energy of ^{3}He transferred to the droplet may be accurately measured by spin-echo experiments [10], while for ^{4}He scattering only bolometric methods would seem feasible.

This work was supported in part by the Austrian Science Fund under grant No. P12832-TPH.

References

1. E. Krotscheck, R. Zillich, J. Chem. Phys. **115**, 10161 (2001)
2. Special Topic: *Helium Nanodroplets: a Novel Medium for Chemistry and Physics*, J. Chem. Phys. **115** (22) 2001
3. J.P. Toennies, in *Microscopic Approaches to Quantum Liquids in Confined Geometries*, edited by E. Krotscheck, J. Navarro (World Scientific, Singapore, 2002), pp. 378–417
4. V. Apaja, E. Krotscheck, in *Microscopic Approaches to Quantum Liquids in Confined Geometries*, edited by E. Krotscheck, J. Navarro (World Scientific, Singapore, 2002), pp. 205–268
5. R.A. Cowley, A.D.B. Woods, Can. J. Phys. **49**, 177 (1971)
6. H.J. Lauter, H. Godfrin, V.L.P. Frank, P. Leiderer, Phys. Rev. Lett. **68**, 2484 (1992)
7. S.A. Chin, E. Krotscheck, Phys. Rev. Lett. **65**, 2658 (1990)
8. R.P. Feynman, Phys. Rev. **94**, 262 (1954)
9. B. Dick, A. Slenczka, J. Chem. Phys. **115**, 10206 (2001)
10. F. Stienkemeier, private communication